

D36

N79-15624

INVESTIGATION OF NONLINEAR MOTION

SIMULATOR WASHOUT SCHEMES

By Susan A. Riedel and L. G. Hofmann

Systems Technology, Inc.

Hawthorne, California

INTRODUCTION

Research interest in washout filters for motion simulator drives arises out of a desire to maximize the fidelity of motion cues presented to simulator pilots. Washout filters must satisfy two important, usually conflicting, requirements:

1. The filter (along with the limiters) must prevent the simulator from reaching the mechanical limits imposed on displacement, velocity and acceleration in each axis.
2. The filter must reproduce actual motion cues without perceptible distortion. That is, motions contributed because of the washout must be imperceptible to the pilot.

The first requirement basically dictates integrated consideration of known motion base limits, existing limiter circuitry and the proposed washout design. The result should be a design which is not at crossed purposes with the limiters. The second requirement, however, demands knowledge of the physiology of motion perception. Research in engineering, physiology and psychology has lead to models of certain mechanisms for motion perception, and has greatly sharpened our knowledge of human motion perception capability. These capabilities (or lack thereof) can then be exploited by the washout designer in fulfilling the second requirement.

The first section of this paper presents an overview of some of the promising washout schemes which have recently been devised. The four schemes presented fall into two basic configurations; crossfeed and crossproduct. Various nonlinear modifications further differentiate the four schemes.

The second section of this paper discusses one nonlinear scheme in detail. This washout scheme takes advantage of subliminal motions to speed up simulator cab centering. It exploits so-called perceptual indifference thresholds to center the simulator cab at a faster rate whenever the input to the simulator is below the perceptual indifference level. The effect is to reduce the angular and translational simulator motion by comparison with that for the linear washout case.

520
A...

The final section of this paper presents the conclusions and implications for further research in the area of nonlinear washout filters.

An Overview of Nonlinear Washout Techniques

All nonlinear washout schemes presented here are modifications to one of the two basic linear designs shown in figure 1. For simplicity, a single set of coupled axes for each design is depicted. The crossproduct scheme, attributed to Schmidt and Conrad (reference 5), is currently implemented on the Large Amplitude Multimode Aerospace Research Simulator (LAMARS) (reference 7). The crossfeed scheme (reference 6) attributed to Bray is implemented on the Flight Simulator for Advanced Aircraft (FSAA) (reference 8).

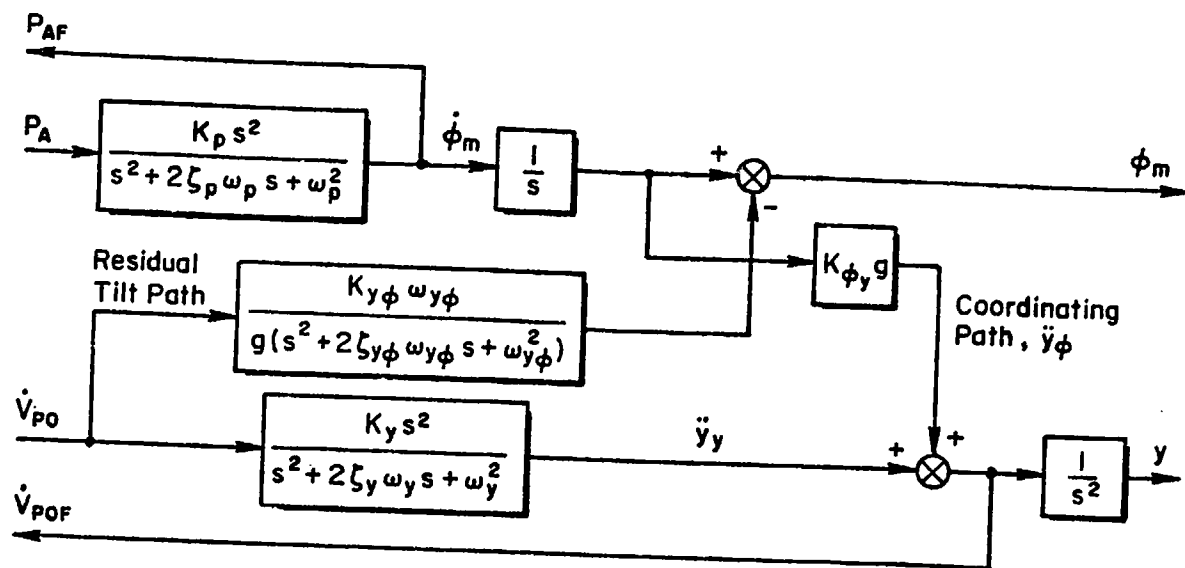
An interesting aspect of the crossproduct scheme is that the recovered specific force always equals the input specific force in the absence of any additional filtering of translational acceleration. In the figures, this implies $\dot{V}_{po} = \dot{V}_{poF}$. This result is due to the configuration of the residual tilt and coordinating crossfeed paths. Notice that because of the different arrangements for the coordinating crossfeed and residual tilt paths in the crossfeed scheme, \dot{V}_{po} and \dot{V}_{poF} are not necessarily equal.

Table 1 compares four nonlinear washout schemes which are in various stages of development. Because of the nonlinear nature of these schemes it is not possible to predict the outcome of a given experiment based on the results of previous experiments. Thus, conclusions drawn from test results for these nonlinear schemes are, at best, tentative.

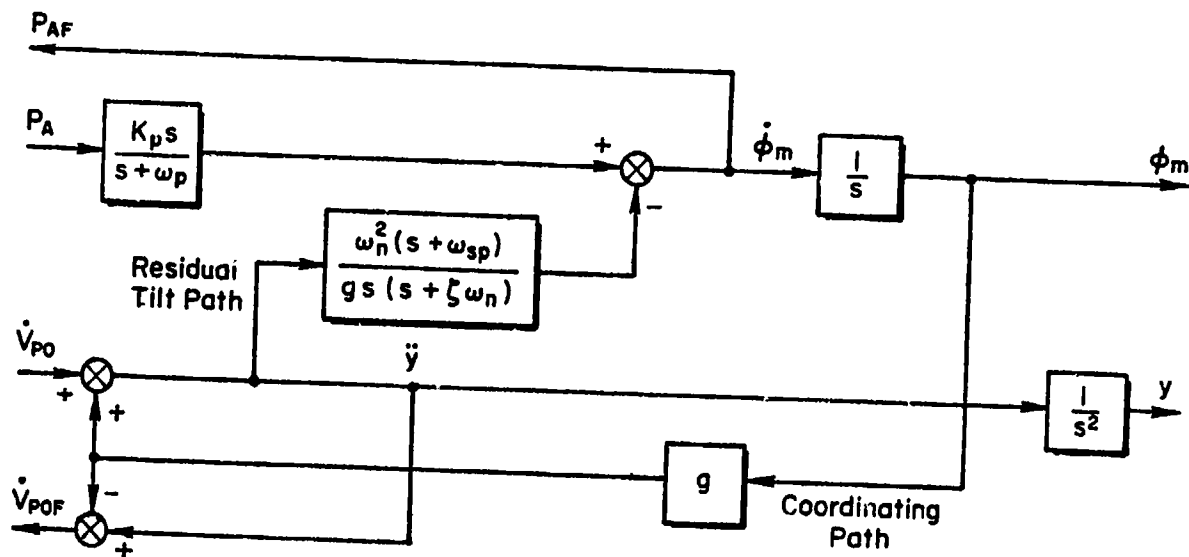
Figure 2 presents a roll axis example of the adaptive gain (Parrish, references 2 and 3) scheme. The gain K_p is computed on-line based upon a cost function. This cost function is a function of roll rate, roll angle and initial K_p . It includes several constants which can be varied to "tune" the filter. The cost function is integrated and limits are imposed to obtain the filter gain. This gain varies with time. When the filter is tuned for a particular application, Parrish and Martin found it helpful for reducing the so-called "false cue" observed in pulse-type maneuvers.

Figure 3 illustrates a sway-axis example of the varying break frequency (Jewell, reference 1) scheme. In this case a cost function is used to compute the time-varying break frequency of the second-order translational washout. The cost function is a function of the translational acceleration, velocity and position as well as break frequency itself. Constants are available to tune the filter. The cost function is then integrated and a limit is imposed to obtain the break frequency. Jewell has demonstrated in a computer simulation that a two-fold reduction in translational motion can be achieved for a quasi-random input.

Figure 4 presents a portion of the surge axis as it appears in a signal compression scheme which incorporates parabolic limiting. While both the Parrish and the Jewell schemes addressed the problem of increased simulation fidelity and decreased motion base requirements, this scheme proposes a solution for the problem of the hardware motion base limits. The essence of this



Crossfeed Scheme - Bray - FSAA



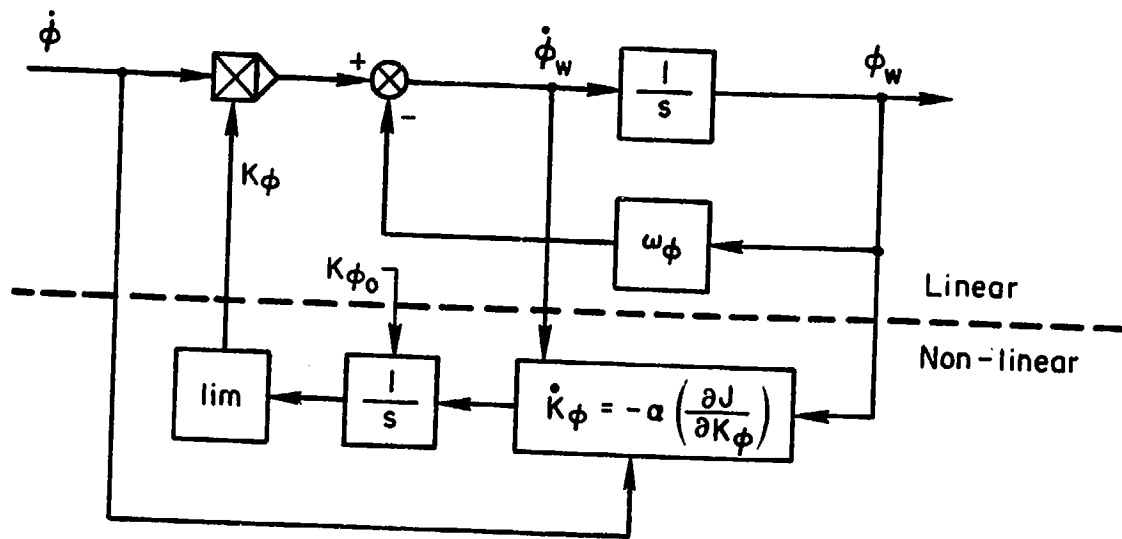
Crossproduct Scheme - Schmidt and Conrad - LAMARS

Figure 1. Basic Single-Axis Linear Washout Circuit Framework

ORIGINAL PAGE IS OF POOR QUALITY

TABLE 1. COMPARISON OF FOUR NONLINEAR WASHOUT SCHEMES

| | <u>Adaptive Gain</u> | <u>Variable Break Frequency</u> | <u>Parabolic Limiting</u> | <u>Subliminal</u> |
|--|--|---|--|---|
| <u>Description</u> | Varies wash-out gain K using a cost function | Varies wash-out break frequency ω_b using a Parrish-type cost function | Incorporated in electrical drive to command maximum deceleration to stop simulator at limits | Increases washout rate when input is subthreshold to force cab back to zero position faster |
| <u>Purpose</u> | Eliminate "false cue" | Reduce motion base displacement requirements | Back-up system for hardware and software units | Reduce motion base displacement requirements |
| <u>Principal Investigators</u> | NASA-Langley Parrish Martin | STI Jewell Jex | NASA-Ames Bray Sinacori | STI Hofmann Riedel |
| <u>Level of Investigation</u> | Implemented on Langley Visual Motion Simulator | Computer model roll-sway axes | Implemented on FSAA | Computer model roll-sway axes |
| <u>Underlying Linear Basis</u> | Crossproduct | Crossproduct | Crossfeed | Crossproduct |
| <u>Inputs for Which Scheme Is Most Effective</u> | Pulse-type inputs | All inputs | Large inputs which could cause limiting | Small, sub-threshold inputs |
| <u>Level of Success</u> | May eliminate "false cues" | Twofold reduction in lateral displacement requirement | Avoids hitting hardware limits | Twofold reduction in lateral displacement requirement |
| <u>Side Effects</u> | Increased nonlinearity with increased motion | Increase in lateral specific force miscoordination | | Increase in lateral specific force miscoordination |
| <u>References</u> | 2, 3 | 1 | 6 | 4 |

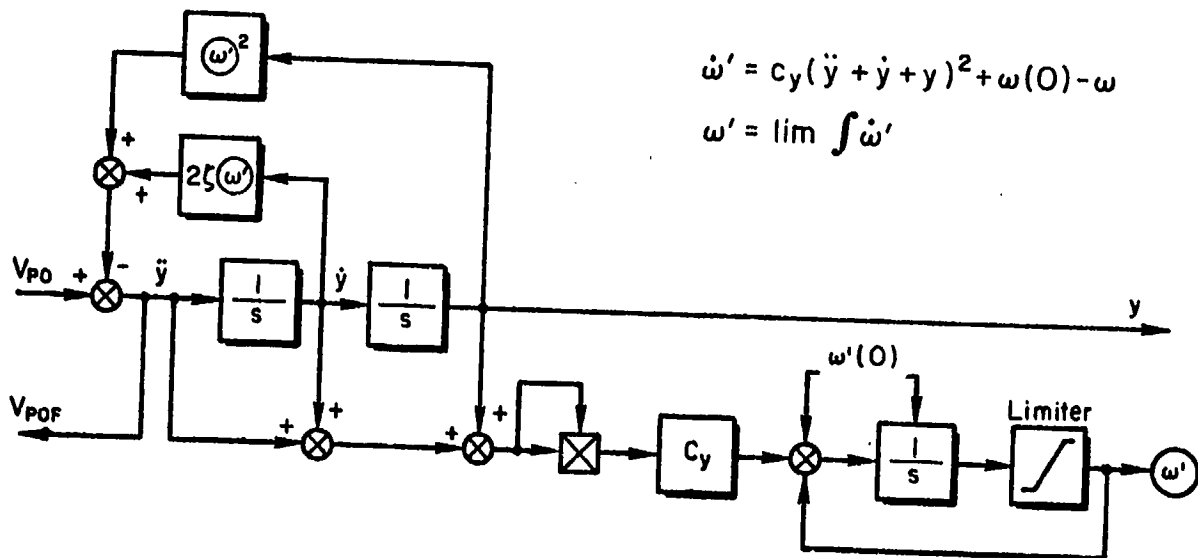


$$\dot{\phi}_w = K_\phi \dot{\phi} - \omega_\phi \phi_w$$

$$\dot{K}_\phi = -\alpha \left(\frac{\partial J}{\partial K_\phi} \right)$$

$$J = 1/2 \left[(\dot{\phi} - \dot{\phi}_w)^2 + b_\phi \phi_w^2 + b_{K_\phi} (K_\phi - K_{\phi_0})^2 \right]$$

Figure 2. Adaptive Gain Scheme



$$\dot{\omega}' = c_y (\ddot{y} + \dot{y} + y)^2 + \omega(0) - \omega$$

$$\omega' = \lim \int \dot{\omega}'$$

Figure 3. Varying Break Frequency Scheme

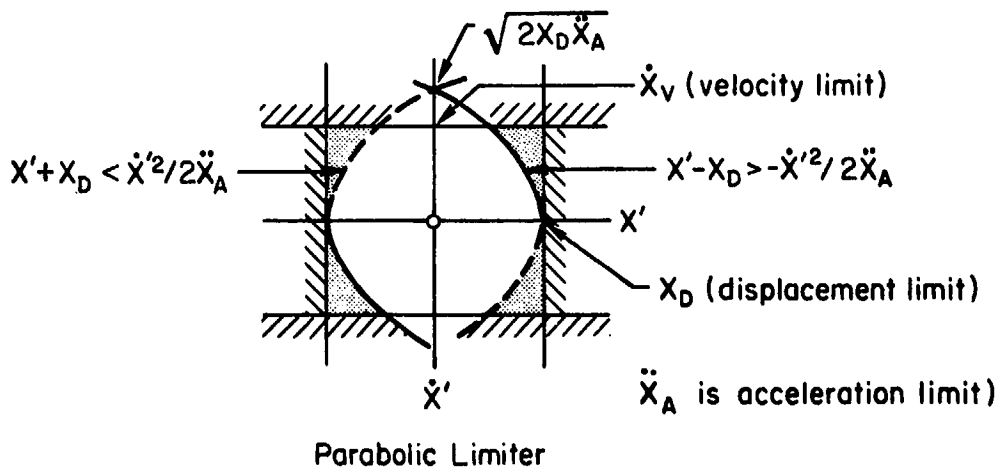
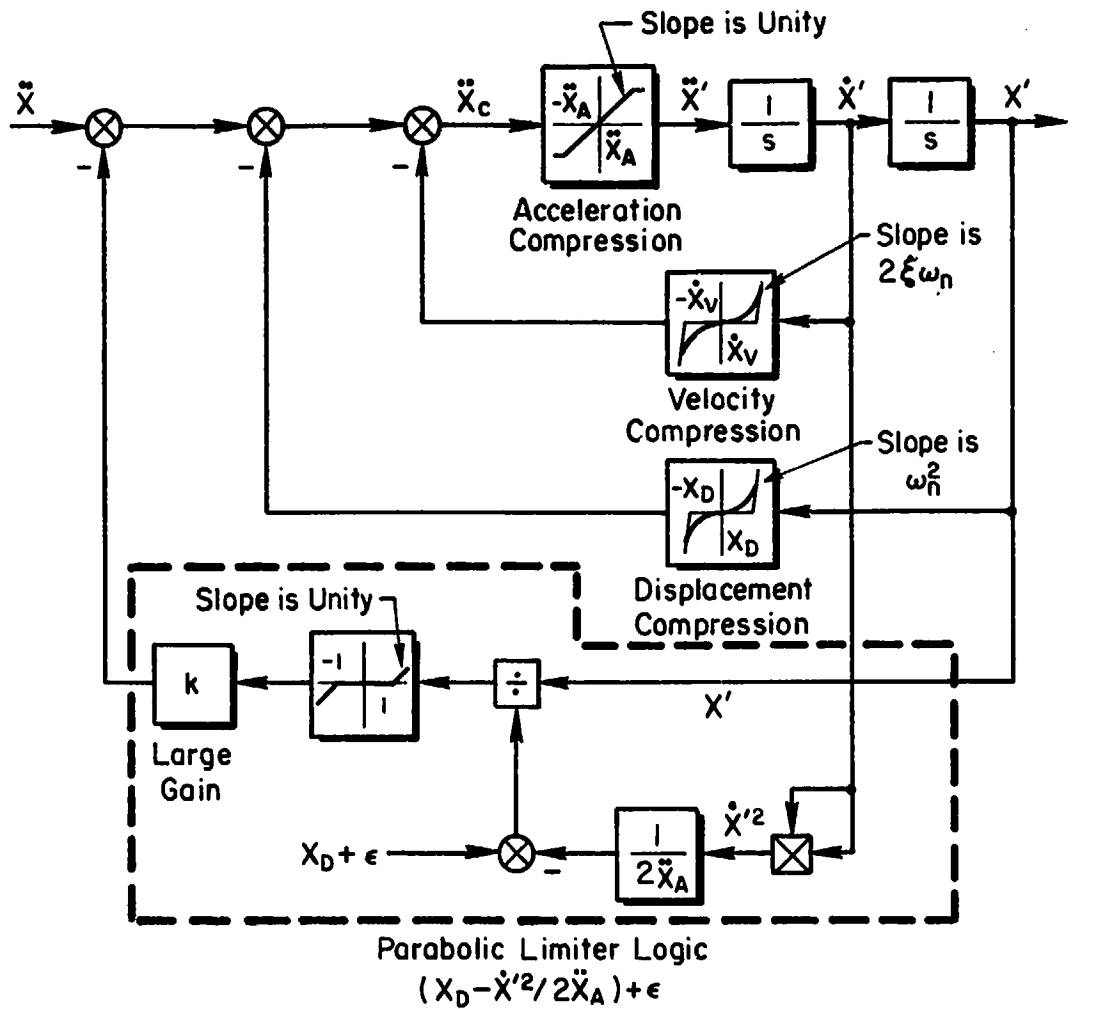


Figure 4. Parabolic Limiting Scheme Incorporating Signal Compression

scheme is a continuous calculation to assure that the cab can be brought to zero velocity before displacement limits are reached. The commanded motion is reproduced to the extent that a margin between the calculated stopping point and the displacement limits exists. In this way, maximum use may be made of the available motion capability.

The fourth washout, the subliminal scheme, is the subject of the next section of this paper.

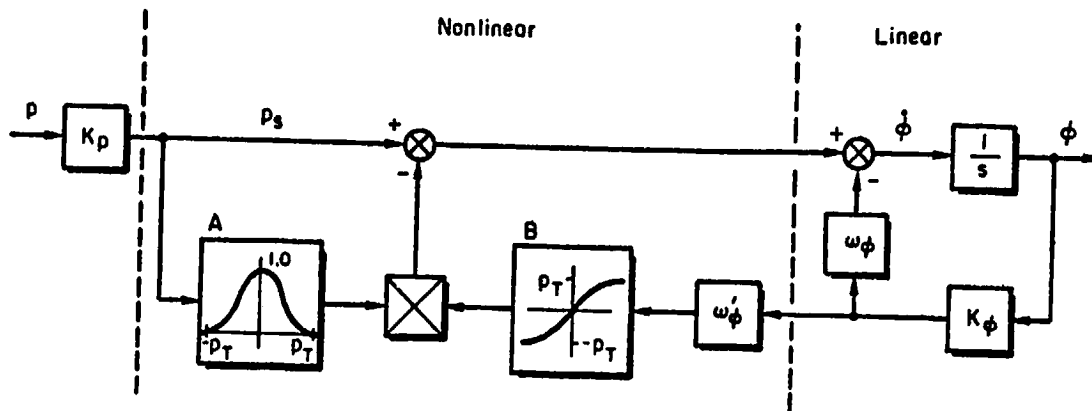
THE SUBLIMINAL WASHOUT SCHEME

Figure 5 presents an application of the subliminal washout scheme to a first-order roll axis washout. This concept came about as the result of an attempt to utilize so-called "indifference" thresholds which pilots exhibit under normal workload. These thresholds may be operative for both angular velocity and specific force perception under normal workload. The hypothesis is that pilots do not perceive angular velocities and specific forces which are below the respective indifference thresholds. The washout design objective is to exploit this particular phenomenon to obtain reduced simulator motion requirements or increased motion fidelity.

The overall design goal is to drive the cab back to its zero position more rapidly than would the underlying linear washout whenever the motion stimulus is below the indifference threshold level. This is accomplished with the use of the two nonlinear functions in boxes A and B in figure 5. The input to the function in Block A is the scaled angular velocity. This function produces a weighting factor which serves as a variable feedback gain in the washout circuit. If the input magnitude is larger than the indifference threshold p_T , the weighting factor is zero. If the input is zero, the weighting factor is 1.0. Otherwise, the weighting factor is some fraction of 1.0 which is a sinusoid-like function of the input for the form of the weighting function used here.

The input to Block B, a soft saturation nonlinear function, is cab roll angle, ϕ . If ϕ is large, the value of the function output is the value of the indifference threshold level, $\pm p_T$. If ϕ is small the value of the function output is proportional to ϕ .

The outputs from Blocks A and B are then multiplied to arrive at an incremental washout rate command signal. The particular choice of functions in Blocks A and B assures that this signal's magnitude never exceeds the indifference threshold level. The smoothness of the functions in Blocks A and B tends to prevent discontinuous commanded changes in the washout rate. The value of this incremental washout rate command signal will be non-zero whenever the cab roll angle is non-zero and the input angular velocity is below the indifference threshold level. The signal is then subtracted from



- p = Input Angular Velocity
- p_s = Scaled Angular Velocity
- p_T = Indifference Threshold Level
- $\dot{\phi}$ = Commanded Cab Roll Rate
- ϕ = Commanded Cab Roll Angle

Figure 5. Nonlinear Washout Scheme (First-order Washout)

the scaled input angular velocity. The result is a smaller away-from-center angular velocity input to the integrator than would result for the underlying linear scheme. Thus, the cab is driven back to its zero position more quickly than it would be for the linear scheme, during intervals of sub-threshold inputs in angular velocity.

Preliminary tests of this subliminal washout concept for the roll axis showed it to be ineffective. There was some reduction in simulator motion requirements, but not really enough to warrant further investigation.

Figure 6 shows an application of this same washout concept to the lateral specific force channel of a crossproduct washout configuration for roll-sway axes.

It was pointed out in the discussion of the crossproduct scheme that the input specific force, V_{po} , and the recovered specific force, V_{poF} , are always equal for the crossproduct washout configuration. In this case the subliminal washout introduces intentional miscoordination of specific force. The indifference phenomenon allows this deliberate introduction of specific force miscoordination, and as long as this miscoordination does not exceed the specific force indifference threshold level, the pilot under normal workload will not detect the miscoordination.

ORIGINAL PAGE IS
OF POOR QUALITY

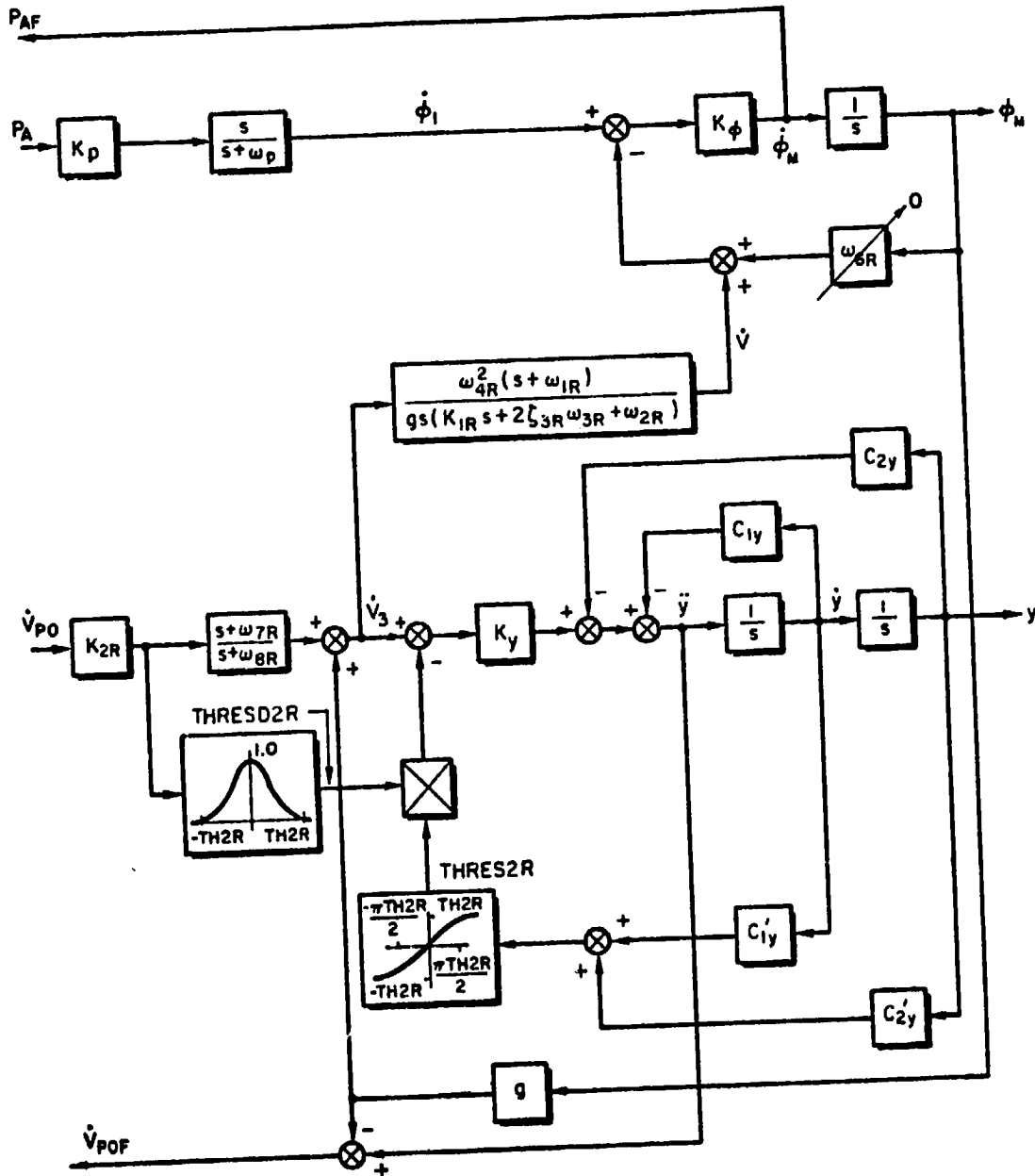


Figure 6. LAMARS Drive Logic Washout with Nonlinear Feedback
Added to Specific Force Path Only

Computer simulation results for the washout in figure 6 are presented in figure 7. The input to the simulation corresponds to a roll-in to a constant 4 g turn. The inputs are roll rate, PA, and lateral specific force, V_{po} . There is no reduction in acceleration, \ddot{y} , slight reduction in velocity, \dot{y} , and significant reduction in lateral translation, y . These results show clearly that the subliminal washout substantially reduces simulator displacement motion requirements. Lateral translation reduction is 70 percent, i.e., from a maximum linear displacement of 4.05 m (13.5 ft) to a maximum displacement of 1.2 m (4 ft).

In order to accomplish this substantial reduction in lateral translational requirements, however, a substantial change in recovered specific force is generated because of miscoordination. This is due to the increased washout rate for the subliminal washout scheme. Since the increase in washout rate is constrained to at or below an indifference threshold level of 0.1 g, the change in recovered specific force is also constrained to that level. Thus, under normal workload the pilot should not be able to detect this level of miscoordination.

The computer simulation of the subliminal washout has been exercised for a variety of inputs. Significant reductions in motion base requirements have been observed. On the basis of these results the following conclusions can be drawn:

1. The subliminal washout concepts, as implemented in the translational axes of the crossproduct scheme, are effective in reducing the velocity and displacement requirements of the motion base.
2. The subliminal washout scheme is most effective for sub-indifference threshold specific force inputs. The washout reduces to the underlying linear scheme when inputs exceed this threshold.
3. The use of the subliminal threshold scheme results in an increase in recovered specific force which is spurious. This spurious motion is due to additional miscoordination. The nonlinear implementation insures that this miscoordination component is never greater than the assumed indifference threshold level. Thus under normal workload, the pilot should be unable to detect this false cue.

Much work remains to be performed in the investigation of this subliminal washout scheme. The initial results of the computer simulation have shed light on the scheme's major uses, and encourage further research and eventual simulator implementation.

ORIGINAL PAGE IS
OF POOR QUALITY

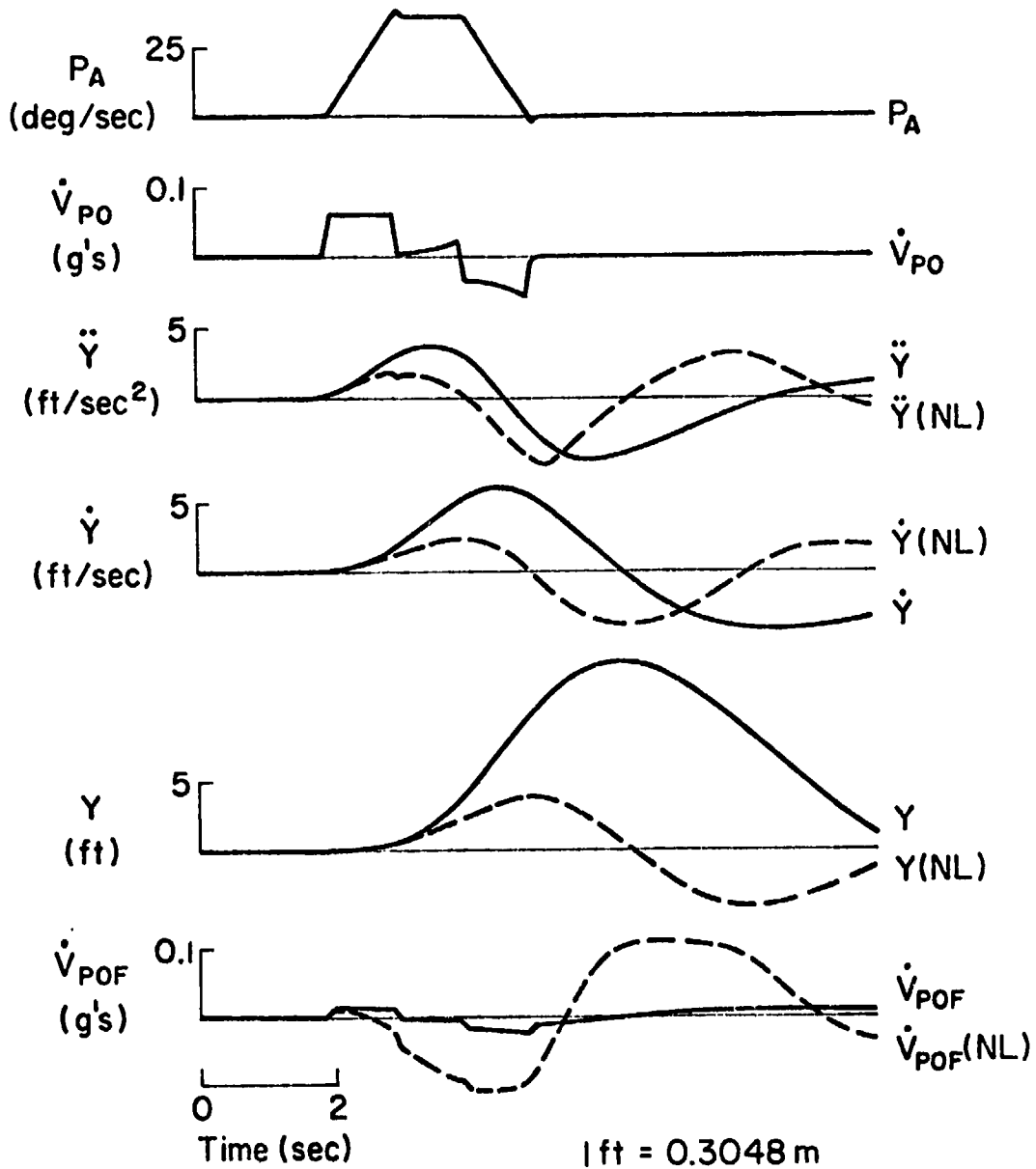


Figure 7. Comparison of Linear and Nonlinear Outputs

CONCLUSIONS

A sample of some new concepts in nonlinear washout filters has been presented here. Since each scheme addresses a different aspect of the washout problem, it may be desirable to combine several nonlinear concepts in a single, grand scheme. In this way, several problems in a particular simulation could be handled by a single washout circuit. Further research along these lines might lead to a well-defined method for designing a washout circuit to suit particular simulation needs, taking into account the peculiarities of the motion base as well as a description of the flying task to be simulated.

The research reported herein was sponsored by the Air Force Flight Dynamics Laboratory under Contract F33615-77-C-2065. (W. Klotzback, AFFDL/FGD and J. Bankovskis, AFFDL/FGD)

REFERENCES

1. Jewell, Wayne F., and Henry R. Jex, "A Second Order Washout Filter With a Time-Varying Break Frequency," STI WP-1094-9, Feb. 1978.
2. Parrish, R. V., and D. J. Martin, Jr., Comparison of a Linear and a Non-linear Washout for Motion Simulators Utilizing Objective and Subjective Data from CTOL Transport Landing Approaches, NASA TN D-8157, 1976.
3. Parrish, R. V., J. E. Dieudonne, R. L. Bowles, and D. J. Martin, "Coordinated Adaptive Washout for Motion Simulators," AIAA Paper No. 73-930, Sept. 1973.
4. Riedel, Susan A., and L. G. Hofmann, "Preliminary Investigation of a New Nonlinear Washout Scheme," STI WP-1110-1, Dec. 1977.
5. Schmidt, S. F., and B. Conrad, Motion Drive Signals for Piloted Flight Simulation, NASA CR-1601, 1970.
6. Sinacori, J. B., "A Brief Survey of Motion Simulators' Drive Logic with Emphasis on the Roll Axis," STI WP-1094-2, May 1977.
7. Sinacori, J. B., "A Practical Approach to Motion Simulation," AIAA Paper No. 73-931, Sept. 1973.
8. Sinacori, J. B., Robert L. Stapleford, Wayne F. Jewell and John M. Lehman, Researchers Guide to the NASA Ames Flight Simulator for Advanced Aircraft (FSAA), STI-TR-1074-1, May 1977.